Searching for stochastic background of light fields with atomic sensors

[...] In this paper, we consider a stochastic background of waves of light fields and measure it by means of a network of precision measurement tools. The past methods (e.g., monochromatic DM wave detection) assumed that the entire energy density of DM (given by the galactic average value) is carried by a monochromatic wave with a frequency fixed at $m_\phi/2\pi$. However, if the total energy density is distributed over a range of frequencies, then the limits summarized in Ref. [1] will be significantly reduced. Therefore, it makes sense to put limits not only on the DM couplings, but also on the spectrum of DM excitations. After analyzing the cases of scalar and vector fields in the context of DM, we also show how similar methodology can be used in the context of gravitational waves.

Scalar fields

We describe the dark matter by a scalar or pseudoscalar field ϕ with mass m_ϕ. We begin with writing down the action (we use the natural units $\hbar = c = 1$ hereafter),

$$S = \int d^4x\sqrt{-g}\left\{\frac{R}{16\pi G} + \frac{1}{2}g_{\mu\nu}\partial^\mu\phi\partial^\nu\phi - V(\phi) + \mathcal{L}_{SM} + \mathcal{L}_{int}\right\}, \tag{1}$$

where G is the Newton's constant, R is the Ricci scalar for the spacetime metric $g_{\mu\nu}$, $V(\phi) = \frac{1}{2}m_\phi^2\phi^2 + \ldots$ is the scalar field potential, $\mathcal{L}_{SM}$ is the Standard Model (SM) Lagrangian and $\mathcal{L}_{int}^{(n)}$ is the interaction Lagrangian, describing the coupling of the ϕ field to the usual matter, that we choose in the standard form of a sum over gauge-invariant operators of SM fields coupled to the powers of ϕ (see, e.g., Refs. [2, 3] for particular cases)

$$\mathcal{L}^{(n)} = \phi\left[\frac{1}{4e^2\Lambda_\gamma}F_{\mu\nu}F^{\mu\nu} - \frac{\beta_{YM}}{2g_{YM}\Lambda_g}G_{\mu\nu}G^{\mu\nu} - \sum_{f=e,u,d}\left(\frac{1}{\Lambda_f} + \frac{\gamma_{m_f}}{\Lambda_g}\right)m_f\bar{\psi}_f\psi_f\right], \tag{2}$$

where $F_{\mu\nu}$ is the standard Maxwell tensor, $G_{\mu\nu}$ is the gluonic field strength tensor, β_{YM} is the beta-function for the running of the SU(3) gauge coupling g_{YM}, γ_{m_f} is the anomalous dimension of the mass operator $\bar{\psi}_f\psi_f$ for the Standard Model fermions ψ_f (for our energy scales we are considering the electron, u- and d-quarks only, see also comments in Ref. [2]). This Lagrangian is chosen in the most general form that is still testable with atomic clocks. Parameters Λ_a are unknowns of dimension of mass describing the strength of the coupling between the scalar field ϕ and Standard Model fields. If Eq. (2) is considered as an effective Lagrangian, then Λ_a describe energy scales for the physics beyond the SM. This particular model is usually considered in the dilaton dark matter studies [2, 6, 7]. For other possible dark matter candidates and couplings (so-called, portals), see [11].

The Lagrangian (2) induces changes in the values of various fundamental constants, such as [2]

$$\frac{\delta\alpha}{\alpha} = \frac{\phi}{\Lambda_\gamma}, \qquad \frac{\delta m_f}{m_f} = \frac{\phi}{\Lambda_f}, \qquad \frac{\delta\Lambda_{QCD}}{\Lambda_{QCD}} = \frac{\phi}{\Lambda_g}, \tag{3}$$

where α is the fine-structure constant and Λ_{QCD} is the QCD mass-scale. It is known that the clock response to the variations of the constants can be expressed as [8]

$$\frac{\delta(\nu/\nu_0)}{\nu/\nu_0} = \frac{\delta V}{V}, \qquad V = \alpha^{K_\alpha}\left(\frac{m_q}{\Lambda_{QCD}}\right)^{K_{q\Lambda}}\left(\frac{m_e}{\Lambda_{QCD}}\right)^{K_{e\Lambda}}, \tag{4}$$

where ν_0 is an arbitrary constant with dimension of frequency, $m_q = (m_u + m_d)/2$ and exponents K_a are either known or can be expressed through other analogous constants for existing atomic clocks, see Refs. [6, 8, 14] and references therein. For the microwave clocks all three exponents contribute due to the dependence of the hyperfine structure constant on the proton and electron masses, in particular, $K_{e\Lambda} = 1$. For the most common frequency standard, ^{133}Cs, $K_\alpha = 2.83$, $K_{q\Lambda} = 0.07$. For optical clocks, $K_{q\Lambda} = K_{e\Lambda} = 0$ and $K_\alpha \neq 0$. Using (3), we obtain

$$\frac{\delta\nu}{\nu} = \phi\left[\frac{K_\alpha}{\Lambda_\gamma} + \frac{K_{q\Lambda}}{\Lambda_q} - \frac{K_{q\Lambda} + K_{e\Lambda}}{\Lambda_g}\right], \quad \Lambda_q \equiv \frac{\Lambda_u\Lambda_d(m_u + m_d)}{m_u\Lambda_d + m_d\Lambda_u}. \tag{5}$$

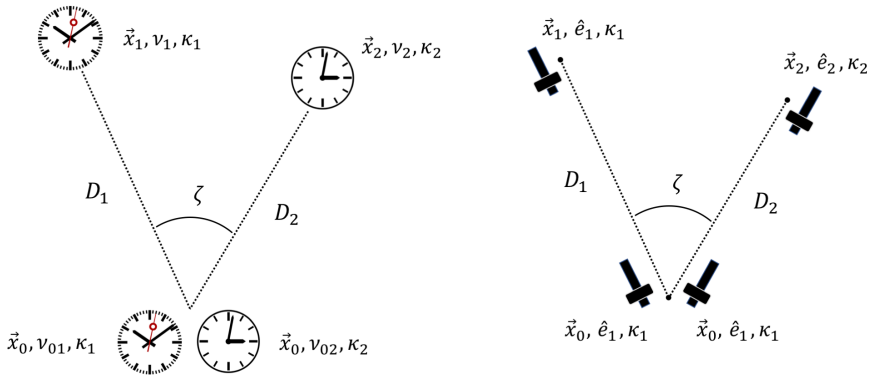

(a) (b)

FIG. 1: (a) Triangle-shaped configuration of two pairs of identical clocks. (b) Triangle-shaped configuration of two pairs of identical atom interferometers pointing in radial direction.

We consider a triangle-shaped configuration of atomic clocks with frequencies ν_i, $i = 01, 02, 1, 2$, placed at positions $\vec{x}_i$, see Fig. 1(a). Each clock responds to the scalar field by a shift in the frequency, $\delta\nu_i$ such as $\delta\nu_i/\nu_i = \kappa_i\phi$. Mass dimension of κ_i is the inverse of the mass dimension of the scalar field, if we assume linear coupling of ϕ to the SM operators. We will measure the difference in the relative frequency shifts, $X_1(t) = \delta\nu_{01}/\nu_{01} - \delta\nu_1/\nu_1$ and $X_2(t) = \delta\nu_{02}/\nu_{02} - \delta\nu_2/\nu_2$. If all three clocks are identical, then these two quantities are simply the difference in the frequencies between clocks "1"/"2" and the reference clock "0". While the configuration of three identical clocks is possible, it will introduce an unwanted correlated noise coming from the reference clock. We will be interested in the cross-spectrum for $X_1(t)$ and $X_2(t)$ and derive a universal dependency of this cross-spectrum on the angle between the pairs of atomic clocks. The idea of the derivation is similar to the calculation of the Hellings-Downs curve [16] for pulsar-timing arrays used in the gravitational wave searches. The scalar field in consideration does not have to be the DM and can be any neutral light scalar field obeying the energy density limit on the hidden matter content in the solar system (or, more generally, in the confining volume of the performed experiment).

In what follows, we assume that the data collection time T is finite but large, giving the frequency resolution of the signal $\Delta f \sim 1/T$. The finite-time Fourier transform for all time-dependent quantities is given by

$$\tilde{X}(f) = T^{-1/2} \int_{-T/2}^{T/2} X(t) e^{-2\pi i f t} dt. \tag{6}$$

We will be replacing the integration limits by infinity, whenever it does not lead to a confusion. The power spectral density $S_X(f)$ of X for one of the clocks is defined via $S_X(f) = |\tilde{X}(f)|^2$ and has the property (Parseval's theorem)

$$\langle X^2(t) \rangle \equiv \lim_{T\to\infty} \frac{1}{T} \int_{-T/2}^{T/2} X^2(t) dt = \int_{-\infty}^{\infty} S_X(f) df \,. \tag{7}$$

We have chosen a two-sided version of the power spectral density to make it easier to change the order of integration, when needed. Notice that the given form of Fourier transform leads to

$$\langle \tilde{X}_1(f) \tilde{X}_2^*(f') \rangle = \frac{1}{T} \delta_T(f - f') S_X(f) \,, \tag{8}$$

where we defined the finite-time delta function as

$$\delta_T(f) \equiv \int_{-T/2}^{T/2} e^{-2\pi i f t} dt = T\mathrm{sinc}(\pi f t)\,. \tag{9}$$

If the two frequencies coincide, then $\delta(0) = T$ cancels the factor T in the denominator and we recover the definition of the power spectrum. Let us consider a stationary isotropic background of scalar field waves. We represent the scalar field as

$$\phi(t,\vec{x}) = \int d^3\vec{k}\,\tilde{\phi}(\vec{k}) e^{i(\vec{k}\cdot\vec{x} - 2\pi f t)}\,, \tag{10}$$

where, in natural units, $2\pi f = (m_\phi^2 + k^2)^{1/2}$. Next, we introduce the cross-spectrum for two sets of clocks comparisons,

$$S_c(f) = \int_{-\infty}^{+\infty} d\tau\, e^{-i2\pi f\tau} \langle X_1(t) X_2(t+\tau)\rangle = \langle \tilde{X}_1(f) \tilde{X}_2^*(f)\rangle\,. \tag{11}$$

We will be using two identities (the second one comes from the isotropic property of the background),

$$\int_{-\infty}^{\infty} df\, S_c(f) = \langle X_1(t) X_2(t)\rangle, \qquad \int_{-\infty}^{\infty} df\, S_\phi(f) = 4\pi \int_0^\infty dk\, k^2 \langle \tilde{\phi}(k)\tilde{\phi}^*(k)\rangle\,, \tag{12}$$

to calculate the cross-spectrum from the power spectrum of the scalar field,

$$\int_{-\infty}^{\infty} df\, S_c(f) = \kappa_1\kappa_2 \int d^3\vec{k} \langle \tilde{\phi}(\vec{k})\tilde{\phi}^*(\vec{k})\rangle \left(1 - e^{i\vec{k}\cdot(\vec{x}_1 - \vec{x}_0)}\right)\cdot\left(1 - e^{-i\vec{k}\cdot(\vec{x}_2 - \vec{x}_0)}\right) = \int_{-\infty}^{\infty} df\, S_\phi(f) R_c(f,\zeta)\,, \tag{13}$$

where the response function $R_c(f,\zeta)$ is given by

$$R_c(f,\zeta) = \frac{\kappa_1\kappa_2}{4\pi} \int_{S^2} d^2\Omega_{\hat{k}} \left(1 - e^{i\vec{k}\cdot(\vec{x}_1 - \vec{x}_0)} - e^{-i\vec{k}\cdot(\vec{x}_2 - \vec{x}_0)} + e^{i\vec{k}\cdot(\vec{x}_1 - \vec{x}_2)}\right)\,. \tag{14}$$

By chosing the appropriate coordinate system (see, e.g., Ref. [17]), one can integrate each term in the sum and obtain

$$R_c(f,\zeta) = \kappa_1\kappa_2 \left[1 - \mathrm{sinc}(kD_1) - \mathrm{sinc}(kD_2) + \mathrm{sinc}(kD_{12})\right]\,, \tag{15}$$

where $D_i \equiv |\vec{x}_i - \vec{x}_0|$, $D_{12} \equiv |\vec{x}_1 - \vec{x}_2|$, and $k = |\vec{k}|$. The response function $R_c(f,\zeta)$ relates the power spectrum of the scalar field fluctuations to the cross-spectrum of the measured signals,

$$S_c(f) = R_c(f,\zeta) S_\phi(f)\,. \tag{16}$$

Since $S_\phi(f)$ is not known *a priori*, from the practical point of view, it makes sense to elminate it by normalizing the cross-spectrum by the power-spectrum of the signal from one pair of atomic clocks, $S_{X_i} = R_i(f) S_\phi(f)$, where $i = 1, 2$, and $R_i(f) = 2\kappa^2\left[1 - \mathrm{sinc}(kD_i)\right]$, see Fig. 2. It is clear from the plot that the sensitivity for a pair of identical atomic clocks reaches its maximum for the separation D_i being larger than the scalar field wavelength. After the normalization of the cross-spectrum, the final result becomes

$$F(f,\zeta) \equiv \frac{S_c(f)}{S_{X_i}(f)} = \frac{\kappa_1\kappa_2}{\kappa_i^2}\cdot\frac{1 - \mathrm{sinc}(kD_1) - \mathrm{sinc}(kD_2) + \mathrm{sinc}(kD_{12})}{2(1 - \mathrm{sinc}(kD_i))}\,. \tag{17}$$

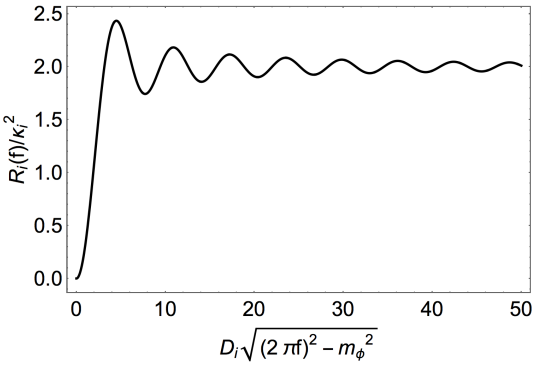

FIG. 2: Response function, $R_i(f)/\kappa_i^2 = 2\,[1 - \mathrm{sinc}(kD_i)]$ for a pair of atomic clocks

.

There are several natural limits greatly simplifying this expression due to the properties of the sinc function,

$$F(f,\zeta) = \begin{cases} \dfrac{\kappa_1\kappa_2}{2\kappa_i^2}, & D_i \gg 1/k, \quad D_{12} \gg 1/k, \\ \dfrac{\kappa_1\kappa_2}{\kappa_i^2}, & D_i \gg 1/k \gg D_{12}, \\ \dfrac{\kappa_1\kappa_2}{\kappa_i^2}\dfrac{D_1 D_2}{D_i^2}\cos\zeta, & D_i \ll 1/k, \end{cases} \tag{18}$$

where ζ is the angle between $(\vec{x}_1 - \vec{x}_0)$ and $(\vec{x}_2 - \vec{x}_0)$. The second limit is geometrically restricted to a situation when $D_1 \approx D_2$ and $\zeta \approx D_{12}/D_i \ll 1$ or, in other words, when $2\pi D_{12}$ is much smaller that the wavelength of the scalar field excitation. It is important to notice that these angular parts do not depend on the DM wave-vectors, frequencies and masses explicitly. Here we used the property $\mathrm{sinc}(a) \approx 0$ when $a \gg 1$ and $\mathrm{sinc}(a) \approx 1 - a^2/6$, when $a \ll 1$. Another nontrivial observation is that the first two limits give us nonzero constants [17], while an uncorrelated noise would give a vanishing cross-correlator.

In the described procedure the frequency of the signal is bounded from below by several factors:

- Mass of the DM field, $f \geq m_\phi/(2\pi)$, due to the dispersion relation for DM.
- The data collection time, T, due to the property of the Fourier transform, so $f \gg 1/T$.
- Time $T_\zeta \sim \Delta\zeta/\dot{\zeta}$ by which the angular distance between sensors changes by the value equal to the uncertainty in the angle ζ. Value of $\Delta\zeta$ should be chosen such that there is enough recorded data for the extraction of the power spectrum density at a given frequency, so $\Delta\zeta \gg \dot{\zeta}/f$.

The maximal frequency is limited by the Nyquist-Shannon-Kotelnikov theorem, $f_{max} = 1/(2\Delta t)$, where Δt is the time interval between consequent measurements. Value of Δt depends on the averaging interval giving desirable performance of the atomic sensors (typically, $\Delta t \geq 1$ s for atomic clocks). Frequencies larger than f_{max} can be studied with the help of aliasing effect.

As an alternative measurement, one can put limits on the unknown combination $\kappa_1\kappa_2 S_\phi(f)$ from the measured cross-spectra at a fixed angle ζ.

The advantage of the cross-spectrum analysis is the cancellation of the uncorrelated noises from individual clocks. However, certain limits can be already put by studying a single clock (with another frequency standard). The clock instability in the time domain can be obtained from the power spectrum of the fractional variation of the clock frequency [19]. Assuming the DM is the dominating source of clock instability, the Allan variance for a clock with response coefficient κ will be given by check

$$\sigma_y^2(\tau) = 2\kappa^2 \int_0^\infty S_\phi(f)\frac{\sin^4(\pi\tau f)}{(\pi\tau f)^2} df\,, \tag{19}$$

where we assumed that the reference frequency standard has a much weaker or no dependence on the DM background. Extracting limits on the DM coupling directly from the clock instability data does not seem possible, due to the lack of knowledge on the DM power spectral density and κ. If, however, the DM spectrum corresponds to a white noise, $S_\phi(f) = \bar{S}_\phi = \text{const}$, and $\sigma_y(\tau) \propto \tau^{-1/2}$, then for SNR=1 we have $\kappa^2 \bar{S}_\phi = 2\tau\sigma_y^2(\tau)$ – a limit on the unknown combination of $\bar{S}_\phi$ and coupling κ. As an example, for a $^{199}\text{Hg}^+$ clock [35] this would mean a bound $\kappa^2 \bar{S}_\phi \leq 3 \times 10^{-29}\,\text{Hz}^{-1}$ and, hence, $\bar{S}_\phi/\Lambda_\gamma^2 \leq 3 \times 10^{-30}\,\text{Hz}^{-1}$.

One can search for the long-wavelength curve (18) in the pulsar timing array data. When passing through a pulsar, the DM wave can change the neutron mass and hence the moment of inertia of the pulsar. This will lead to the variation of the pulsar rotation period. For the sensitivity estimates in a case of a single monochromatic DM wave, see Ref. [11].

Vector fields

Another popular DM candidate is the massive $B-L$ vector field that acts differently on species with different neutron content. This field can be probed in experimental tests of the weak equivalence principle and manifests itself in an additional relative acceleration between two particle species a and b [11]

$$\Delta\vec{a}_{B-L}(t,\vec{x}) = \frac{g_{B-L}}{m_N}\left(\frac{Z_a}{A_a} - \frac{Z_b}{A_b}\right)\vec{W}(t,\vec{x}) \equiv \kappa\vec{W}(t,\vec{x})\,, \tag{20}$$

where g_{B-L} is the coupling constant to the $B-L$ field $\vec{W}$, $Z_{a,b}$ and $A_{a,b}$ are the atomic numbers and weights, respectively, m_N is the neutron mass, and we also introduced the constant κ for the sake of compactness. Let us consider four atom interferometers (AI) in a triangle-shaped configuration, such that two of them are at the position $\vec{x}_0 = 0$ and the other two are at the positions $\vec{x}_1$ and $\vec{x}_2$, respectively, see Fig. 1(b). All AI are oriented in the radial direction with respect to the center at $\vec{x}_0$. The quantities we are interested in are defined by

$$X_i(t) = \Delta\vec{a}_{B-L}(t,\vec{x}_0) - \Delta\vec{a}_{B-L}(t,\vec{x}_i) = \kappa_i\hat{e}_i\cdot(\vec{W}(t,\vec{x}_0) - \vec{W}(t,\vec{x}_i))\,, \tag{21}$$

where $\hat{e}_i$ are unit vectors oriented along the AI. We represent the vector field W as

$$\vec{W}(t,\vec{x}) = \int d^3\vec{k} \sum_{i=1,2,3} \tilde{W}_i(\vec{k})\hat{\epsilon}_i(\hat{k})\, e^{i(\vec{k}\cdot\vec{x} - 2\pi f t)}\,, \tag{22}$$

where $\hat{\epsilon}_i(\hat{k})$ are polarization vectors, such as $\hat{\epsilon}_i(\hat{k})\cdot\hat{\epsilon}_j(\hat{k}) = \delta_{ij}$ and the dispersion relation is $2\pi f = (m_W^2 + k^2)^{1/2}$ with m_W being the mass of the $B-L$ field. We further consider a stochastic, isotropic and unpolarized background of vector waves characterized by the power spectrum density $S_W(f)$,

$$\langle\tilde{W}_i(\vec{k})\tilde{W}_j^*(\vec{k})\rangle = \frac{1}{3}S_W(f)\delta_{ij}, \qquad \langle\vec{W}^2(t,\vec{x})\rangle = \int\limits_{-infty}^{\infty} S_W(f)\,df\,. \tag{23}$$

Notice the factor 3 in the denominator, which shows the number of physical polarizations. In analogy with the previous section, we calculate the cross-spectrum, $S_c(f) = R_c(f,\zeta)S_W(f)$, where

$$R_c(f,\zeta) = \frac{\kappa_1\kappa_2}{4\pi}\int_{S^2} d^2\Omega_{\hat{k}}\,\frac{1}{3}\sum_{i=1,2,3}\left[\hat{e}_1\cdot\hat{\epsilon}_i(\hat{k})\right]\left[\hat{e}_2\cdot\hat{\epsilon}_i(\hat{k})\right]\left(1 - e^{i\vec{k}\cdot\vec{x}_1}\right)\cdot\left(1 - e^{-i\vec{k}\cdot\vec{x}_2}\right)\,. \tag{24}$$

To compute this integral we first fix the orientations of AI in the Cartesian (x,y,z)-coordinates,

$$\hat{e}_1 = \hat{z}, \qquad \hat{e}_2 = \sin\zeta\,\hat{x} + \cos\zeta\,\hat{z}\,, \tag{25}$$

and then fix the orthonormal basis of polarization vectors in polar coordinates (k,θ,φ),

$$\hat{\epsilon}_1(\hat{k}) = \cos\theta\cos\varphi\,\hat{x} + \cos\theta\sin\varphi\,\hat{y} - \sin\theta\,\hat{z} = \hat{\theta}, \tag{26}$$

$$\hat{\epsilon}_2(\hat{k}) = -\sin\varphi\,\hat{x} + \cos\varphi\,\hat{y} = \hat{\varphi}, \tag{27}$$

$$\hat{\epsilon}_3(\hat{k}) = \sin\theta\cos\varphi\,\hat{x} + \sin\theta\sin\varphi\,\hat{y} + \cos\theta\,\hat{z} = \hat{k}. \tag{28}$$

In the short-wavelength approximation, $D_i, D_{12} \gg 1/k$, we can neglect the exponents in the right-hand side of (24) and obtain $R_c(f,\zeta) = \frac{\kappa_1\kappa_2}{3}\cos\zeta$. If $D_i \gg 1/k, D_{12} \ll 1/k$, then $R_c(f,\zeta) = \frac{2\kappa_1\kappa_2}{3}\cos\zeta$, similar to the previous section. Finally, in the long-wavelength limit, $D_i \ll 1/k$, taking into account that $\hat{x}_i = \hat{e}_i$ and expaning the exponent in series, we get $R_c(f,\zeta) = \frac{\kappa_1\kappa_2}{9}k^2 D_1 D_2 \cos^2\zeta$. Considering the power spectrum for each individual pair of AI, $S_{X_i}(f) = R_i(f)S_W(f)$, we obtain $R_i(f) = \frac{2}{3}\kappa_i^2$ if $D_i \gg 1/k$ and $R_i(f) = \frac{\kappa_i^2}{15}(kD_i)^2$ if $D_i \ll 1/k$. Finally, introducing the angular curve $F(f,\zeta) \equiv S_c(f)/S_{X_i}(f)$ we summarize the results of this section:

$$F(f,\zeta) = \begin{cases} \dfrac{\kappa_1\kappa_2}{2\kappa_i^2}\cos\zeta, & D_i \gg 1/k, \quad D_{12} \gg 1/k, \\ \dfrac{\kappa_1\kappa_2}{\kappa_i^2}\cos\zeta, & D_i \gg 1/k \gg D_{12}, \\ \dfrac{5}{3}\dfrac{D_1 D_2}{D_i^2}\dfrac{\kappa_1\kappa_2}{\kappa_i^2}\cos^2\zeta, & D_i \ll 1/k, \end{cases} \tag{29}$$

so the strategy of detecting the DM footprint in the data is to search for a cosine or cosine squared modulation of the normalized cross-spectra. If the vector field excitation is gapless, then the number of physical polarizations is reduced to two and the problem resembles the case of electromagnetic stochastic background [17].

Tensor fields

In this section we discuss an application of the method to the searches of isotropic stationary gravitational wave (GW) background. An example of the configuration is depicted in Fig. 1(a), where the atomic clocks are placed in spacecrafts or attached to celestial bodies in free fall. Synchronization of the clocks is performed with an electromagnetic signal (e.g., laser) with frequency locked to the frequency of one of the clocks in the pair, see, e.g., proposals in Refs. [28, 29]. The frequency difference due to the presence of the GW is denoted $X_a = \delta\nu_a/\nu_a$. Our goal, as before, is to extract the angular part of the cross-spectrum, $R_c(f,\zeta)$. The small perturbation of the metric around the Minkowski metric $\eta_{\mu\nu}$ is given by $g_{\mu\nu} = \eta_{\mu\nu} + h_{\mu\nu}$. The metric perturbation $h_{\mu\nu}$ in a spatial transverse traceless gauge has $h_{0\mu} = 0$ and can be represented by the plane wave expansion [20]

$$h_{ij}(t,\vec{x}) = \int_{-\infty}^{\infty} df \int_{S^2} d\hat{\Omega}\, e^{i2\pi f(t-\hat{\Omega}\cdot\vec{x})} \sum_{P=+,\times} h_P(f,\hat{\Omega}) e_{ij}^P(\hat{\Omega})\,, \tag{30}$$

where f is the frequency of the wave, unit vector $\hat{\Omega}$ points in the direction of the propagation of the plane-wave component. Dispersion relation for the gravitational waves is simply $2\pi f = k$. The polarization tensors can be defined through unit vectors $\hat{n}$ and $\hat{m}$ orthogonal to $\hat{\Omega}$,

$$e_{ij}^+(\hat{\Omega}) = \hat{m}_i\hat{m}_j - \hat{n}_i\hat{n}_j, \quad e_{ij}^\times(\hat{\Omega}) = \hat{m}_i\hat{n}_j + \hat{n}_i\hat{m}_j\,, \tag{31}$$

where in the standard spherical coordinates

$$\hat{\Omega} = (\sin\theta\cos\phi, \sin\theta\sin\phi, \cos\theta), \tag{32}$$

$$\hat{m} = (\sin\phi, -\cos\phi, 0), \tag{33}$$

$$\hat{n} = (\cos\theta\cos\phi, \cos\theta\sin\phi, -\sin\theta). \tag{34}$$

We begin from considering an effect of a single plane wave propagating in direction $\hat{\Omega}$ on a signal sent between atomic clocks separated by distance D_a. The unit vector $\hat{p}_{(a)}$ is pointing from the observation point to the singnal source. In order to find the Doppler shift X_a, one can consider the null vector[24]

$$\sigma_{(a)}^\mu = s_{(a)}^\mu - \frac{1}{2}\eta^{\mu\alpha}h_{\alpha\beta}s_{(a)}^\beta\,, \tag{35}$$

at the moments when the signal is emmited and received, with the unperturbed value given by $s^\mu_{(a)} = \nu(1, -\hat{p}_{(a)})$. The null geodesics can be found by solving the null condition $\sigma_{\mu(a)}\sigma^\mu_{(a)} = 0$ together with the standard condition $\sigma_\mu V^\mu_{(a)} = \text{const}_{(a)}$, where $V^\mu_{(a)}$ are the Killing vectors for the perturbed geometry. The final result is given by

$$X_a(t) = \frac{1}{2}\sum_{P,i,j} \frac{\hat{p}^i_{(a)}\hat{p}^j_{(a)} e^P_{ij}}{1 + \hat{\Omega}\cdot\hat{p}_{(a)}} \left(h_P\left[t - \left(1 + \hat{\Omega}\cdot\hat{p}_{(a)}\right) D_a\right] - h_P[t]\right) , \tag{36}$$

where we take into account the isotropic nature of the radiation and consider the perturbation amplitudes as functions of light-cone coordinates. The power spectrum density for the induced Doppler shifts, $S_{X_a}(f) = \langle \tilde{X}_a(f)\tilde{X}^*_a(f)\rangle$ is given by averaging over time, directions $\hat{\Omega}$ and polarizations of the incoming radiation. It can be shown that $S_{X_a}(f) = R_a(f)S_h(f)$, where the GW power spectral density is defined by $\langle \tilde{h}_P(f)\tilde{h}^*_{P'}(f)\rangle = \frac{1}{2}S_h(f)\delta_{PP'}$ and the response function is given by

$$R_a(f) = \frac{1}{3} - \frac{1}{8(\pi D_a f)^2} + \frac{\sin(4\pi D_a f)}{32(\pi D_a f)^3}, \tag{37}$$

see Fig. 3(a). In a long wavelength limit, $2\pi f D_a \ll 1$, the response function reduces to $R_a(f) = \frac{4\pi^2}{15}(D_a f)^2$, while in the short wavelength limit it is simply $R_a(f) = 1/3$. By considering Eq. (36) in the Fourier space, one can derive the cross-spectrum, $S_c(f) = \langle \tilde{X}_1(f)\tilde{X}^*_2(f)\rangle = R_c(f,\zeta)S_h(f)$, where

$$\begin{aligned} R_c(f,\zeta) =& \frac{1}{4\pi}\int\limits_{S^2} d\hat{\Omega}\left(e^{2\pi i f D_1\left(1+\hat{\Omega}\cdot\hat{p}_{(1)}\right)} - 1\right)\left(e^{-2\pi i f D_2\left(1+\hat{\Omega}\cdot\hat{p}_{(2)}\right)} - 1\right) \\ &\times \frac{1}{8}\sum_{i,j,l,m,P} \frac{\hat{p}^i_{(1)}\hat{p}^j_{(1)}e^P_{ij}}{1+\hat{\Omega}\cdot\hat{p}_{(1)}} \cdot \frac{\hat{p}^l_{(2)}\hat{p}^m_{(2)}e^P_{lm}}{1+\hat{\Omega}\cdot\hat{p}_{(2)}} \end{aligned} \tag{38}$$

In order to perform the direction averaging for the radiation background, we chose the z-axis to be along $\hat{p}_{(1)}$ and $\hat{p}_{(2)}$ to have an angle ζ with respect to $\hat{p}_{(1)}$, similar to the previous section,

$$\hat{p}_{(1)} = (0,0,1), \qquad \hat{p}_{(2)} = (\sin\zeta, 0, \cos\zeta). \tag{39}$$

The angular dependency on ζ in the power spectrum density $S_c(f)$ can be factorized in the short-wavelength limit, $D_a, D_{12} \gg 1/k$ and corresponds to the Hellings-Downs curve[16, 25] used in the pulsar timing studies,

$$R_c(f,\zeta) = \frac{1}{3} + \frac{1}{2}(1-\cos\zeta)\left[\ln\left(\frac{1-\cos\zeta}{2}\right) - \frac{1}{6}\right], \qquad D_a, D_{12} \gg 1/k\,. \tag{40}$$

To calculate this expression, one can neglect exponents in Eq. (38), since their arguments are quickly oscillating functions of spherical angles. When $D_a \gg 1/k$, but $D_{12} \ll 1/k$, one will get the same result multiplied by factor 2, as in the previous sections. In the opposite limit, $D_a \ll 1/k$, on can expand the exponents in series and obtain

$$R_c(f,\zeta) = \frac{\pi}{8}\int\limits_{S^2} d\hat{\Omega}\, f^2 D_1 D_2 \sum_{i,j,l,m,P} \hat{p}^i_{(1)}\hat{p}^j_{(1)}\hat{p}^l_{(2)}\hat{p}^m_{(2)}e^P_{ij}e^P_{lm} = \frac{\pi^2 f^2}{15} D_1 D_2 (1 + 3\cos 2\zeta)\,, \tag{41}$$

which reproduces the response function of one pair of atomic clocks in this limit, when $\zeta = 0$. One can notice that the angular function above is proportional to the second Legendre polynomial, $P_2(\cos\zeta)$, which one can expect from the expansion of the background by spherical harmonics [26, 27]. Finally,

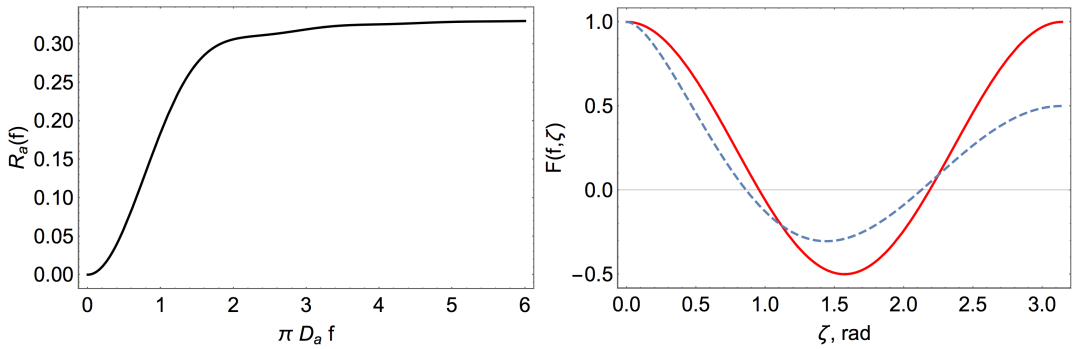

(a) (b)

FIG. 3: (a) The response function, Eq. (37); (b) Normalized angular part of the cross-spectrum in the short-wavelength (dashed line) and long-wavelength (solid line) limits, Eq. (42)

introducing, again, the angular curve $F(f,\zeta) \equiv S_c(f)/S_{X_i}(f)$ we conclude this section,

$$F(f,\zeta) = \begin{cases} 1 + \dfrac{3}{2}(1-\cos\zeta)\left[\ln\left(\dfrac{1-\cos\zeta}{2}\right) - \dfrac{1}{6}\right], & D_i \gg 1/k, \quad D_{12} \gg 1/k, \\ 2 + (1-\cos\zeta)\left[3\ln\left(\dfrac{1-\cos\zeta}{2}\right) - \dfrac{1}{2}\right], & D_i \gg 1/k \gg D_{12}, \\ \dfrac{D_1 D_2}{4D_i^2}(1+3\cos 2\zeta), & D_i \ll 1/k, \end{cases} \tag{42}$$

We plot the first and the third curves in Fig. 3(b) assuming $D_1 = D_2$. Sensitivity of a subsystem of a pair of atomic sensors is discussed in Refs. [28, 29].

DM wind

DM direct detection experiments should take into account the possibility of DM moving with a constant velocity $\vec{v}_b$ with respect to the observer (DM "wind"), see Ref. [18] and refs. therein. Since the solar system moves through the galactic halo of the DM, such velocity may be given by the velocity of the Sun with respect to the galactic rest frame. If the solar system has its own DM halo, then the velocity of DM with respect to the near-earth experiment would be given by the Earth orbital speed. In this section, we consider the effect of the constant motion of the confuguration of detectors through the DM rest frame without making assumptions on the particular direction and absolute value of such constant velocity. Our goal is to see the change in the angular part of cross-spectra when the velocities of DM waves are shifted by a constant vector $\vec{v}_b$.

For the scalar excitations, due to the properties of the Fourier transformation,

$$\langle\tilde{\phi}(\vec{k})\tilde{\phi}^*(\vec{k}-\vec{k}_b)\rangle = \langle\tilde{\phi}(\vec{k}-\vec{k}_b)\tilde{\phi}^*(\vec{k})\rangle = S_\phi(f')\,, \tag{43}$$

where $\vec{k}_b \equiv m_\phi \vec{v}_b$, S_ϕ is the isotropic power spectrum and $f' = (m_\phi^2 + (\vec{k}-\vec{k}_b)^2)^{1/2}/(2\pi)$ is the Doppler-shifted frequency of the stochastic excitations. The response functions $R = R(f')$ can be calculated by considering the shifted wave-vectors, $\vec{k} = \vec{k}_b + \vec{k}'$,

$$R_c(f',\zeta) = \frac{\kappa_1\kappa_2}{4\pi}\int_{S^2} d^2\Omega_{\hat{k}}\left(1 - e^{i(\vec{k}_b+\vec{k}')\cdot\vec{x}_1} - e^{-i(\vec{k}_b+\vec{k}')\cdot\vec{x}_2} + e^{i(\vec{k}_b+\vec{k}')\cdot(\vec{x}_1-\vec{x}_2)}\right). \tag{44}$$

where we consider the configuration given by Fig. 1(a), and $\vec{x}_0 = 0$, for the sake of simplicity. After the integration, the expression becomes

$$R_c(f',\zeta) = \kappa_1\kappa_2\left[1 - \mathrm{sinc}(|\vec{k}'+\vec{k}_b|D_1) - \mathrm{sinc}(|\vec{k}'+\vec{k}_b|D_2) + \mathrm{sinc}(|\vec{k}'+\vec{k}_b|D_{12})\right], \tag{45}$$

giving us familiar results,

$$F(f,\zeta) = \begin{cases} \dfrac{\kappa_1\kappa_2}{2\kappa_i^2}, & D_i, D_{12} \gg 1/\max(k', k_b), \\ \dfrac{\kappa_1\kappa_2}{\kappa_i^2}, & D_i \gg 1/\max(k', k_b) \gg D_{12}, \\ \dfrac{\kappa_1\kappa_2}{2\kappa_i^2}\dfrac{D_1 D_2}{D_i^2}\cos\zeta, & D_i \ll 1/\max(k', k_b), \end{cases} \tag{46}$$

To summarize the strategy, if the normalized cross-spectra give a constant (e.g., 1 or 1/2, for identical clocks) or cosine dependence on the angle between two pairs of atomic clocks, then the measured signal may be dominated by the presence of a new scalar field.

The same logic can be applied to the vector excitations measured with AI, and the result repeats Eq. (29) with k being replaced by $\max(k', k_b)$ in the limits.

Signal-to-noise ratio and statistical inference

In this section we provide the signal-to-noise ratio (SNR) for the stochastic background measurement, optimal filter, as well as the probability of the presence of the signal in the noise. Our derivations are inspired by the gravitational wave detection methods [20–22], for the basics of the signal extraction from noise see, e.g., Ref. [23]. We focus on the case of scalar fields, the generalization on other cases is straightforward. We consider the measured observable as a sum of a (weak) signal $\phi(t)$ and a noise $n(t)$, both having zero expectation values. For each pair of atomic clocks the noise is characterized by the (one-sided) power spectrum S_{n_i}, and the noises are assumed to be uncorrelated and stationary. In order to solve the problem of optimal filtering, we consider the signal to be

$$S \equiv \frac{1}{T}\int\limits_{-T/2}^{T/2} dt \int\limits_{-T/2}^{T/2} dt'\, s_1(t) s_2(t') Q(t-t')\,. \tag{47}$$

If the filter $Q(t-t') = \delta(t-t')$, then the signal is simply $S = \langle \phi_1(t)\phi_2(t)\rangle$. This signal can be, however, buried under noise and we need to construct a filter $Q(t)$ that will maximize SNR, eventually making it large enough by the expense of long observation time T. It will be shown that SNR $\sim \sqrt{T}$ for our measurement. The Fourier space representation of the signal is

$$S = \int\limits_{-\infty}^{\infty} df \int\limits_{-\infty}^{\infty} df'\, \delta_T(f-f')\tilde{s}_1^*(f)\tilde{s}_2(f')\tilde{Q}(f')\,, \tag{48}$$

where we assumed that $Q(\tau)$ decays quickly with $\tau \to \pm\infty$. Next, the statistical properties of the field amplitudes and the noise can be expressed as

$$\langle \tilde{\phi}_1^*(f)\tilde{\phi}_2(f')\rangle = \frac{1}{T}\delta_T(f-f')F(f,\zeta)S_\phi(f)\,, \tag{49}$$

$$\langle \tilde{n}_1^*(f)\tilde{n}_2(f')\rangle = \frac{1}{2T}\delta_T(f-f')\delta_{ij}S_{n_i}(|f|)\,. \tag{50}$$

and, in addition to the property $\delta_T(0) = T$, lead to

$$\langle S\rangle = \int\limits_{-\infty}^{\infty} df\, F(f,\zeta)S_\phi(f)\tilde{Q}(f)\,. \tag{51}$$

The noise is defined in the standard way, $N \equiv S - \langle S \rangle$. Assuming the noise contributions dominate the signal, we can write

$$N \simeq \int\limits_{-\infty}^{\infty} df \int\limits_{-\infty}^{\infty} df' \, \delta_T(f - f') \tilde{n}_1^*(f) \tilde{n}_2(f') \tilde{Q}(f') \,, \tag{52}$$

and further obtain

$$\langle N^2 \rangle = \langle S^2 \rangle - \langle S \rangle^2 \simeq \frac{1}{4T} \int\limits_{-\infty}^{\infty} df \, S_{n_1}(|f|) S_{n_2}(|f|) |\tilde{Q}(f)|^2 \,, \tag{53}$$

where we used a standard way of expressing the 4th moment through the covariances and took into account that $\int\limits_{-\infty}^{\infty} \delta_T^2(f - f') df' = T$ at large T. Comparing this expression to Eq. (51), one can see that $\mathrm{SNR}^2 = \langle S \rangle^2 / \langle N^2 \rangle$ is maximized at

$$\tilde{Q}(f) = \frac{F(f, \zeta) S_\phi(f)}{S_{n_1}(|f|) S_{n_2}(|f|)} \tag{54}$$

and gives

$$\mathrm{SNR}^2 \simeq 8\, T \int\limits_0^{\infty} \frac{F^2(f, \zeta) S_\phi^2(f)}{S_{n_1}(f) S_{n_2}(f)} df \,. \tag{55}$$

Notice that $\mathrm{SNR} \propto \sqrt{T}$ and the noise decreases with more data points, so, in ideal conditions, an arbitrarily small signal can be extracted from noise for large duration of the observation. In order to detect a weak signal, one has to assume a certain shape of the spectrum $S_\phi(f)$, false alarm rate α and false dismissal rate β. Consider a set of measurements $\{S_i\}$, each of duration T. The Neyman-Pearson decision criterion (maximized probability of the detection with fixed alarm rate α) allows to choose the null hypothesis if $\sqrt{n}\, \hat{\mathrm{SNR}} < \sqrt{2}\, \mathrm{erfc}^{-1}(2\alpha)$ and claim the presence of the DM signal of unknown amplitude if $\sqrt{n}\, \hat{\mathrm{SNR}} \leq \sqrt{2}\, \mathrm{erfc}^{-1}(2\alpha)$, where n is the (large) number of statistically independent measurements, $\hat{\mathrm{SNR}} \equiv \langle S \rangle / \sqrt{\langle (S - \langle S \rangle)^2 \rangle}$ is the measured signal-to-noise ratio and $\mathrm{erfc}^{-1}(x)$ is the inverse of the complementary error function.

Assuming the signal is present in the data, the theoretical SNR required for the detection of the DM background in at least $(1 - \beta) \times 100\%$ of measurements is given by (should I provide more details?)

$$\sqrt{n} \mathrm{SNR} \geq \sqrt{2} \left[\mathrm{erfc}^{-1}(2\alpha) - \mathrm{erfc}^{-1}(2 - 2\beta) \right] \,. \tag{56}$$

If the spectrum is flat, $S_\phi(f) = \bar{S}_\phi = \mathrm{const}$, in order to detect the signal, one would require the following minimal value of $\bar{S}_\phi$,

$$\bar{S}_\phi \geq \frac{1}{2\sqrt{nT}} \left[\int\limits_0^{\infty} df \frac{F^2(f, \zeta)}{S_{n_1}(f) S_{n_2}(f)} \right]^{-1/2} \times \left[\mathrm{erfc}^{-1}(2\alpha) - \mathrm{erfc}^{-1}(2 - 2\beta) \right] \,. \tag{57}$$

Same technique can be applied to a network of more that two pairs of clocks, see Ref. [20] discussing it in the context of gravitational wave detectors. For the anisotropic backgrounds and real data complications see, e.g., Ref. [22]. For illustration purposes, let us consider a system of identical clocks in the short-wavelength regime ($F = 1/2$), with the scalar field background being localized around frequency f_0 in a narrow band Δf and, for the particular statistics $\alpha = \beta = 0.05$. Then the mentioned above expressions are simplified to

$$\mathrm{SNR} = \frac{\bar{S}_\phi \sqrt{2T\Delta f}}{S_n(f_0)}, \qquad \bar{S}_\phi^{5\%,5\%} \geq \frac{2.33\, S_n(f_0)}{\sqrt{nT\Delta f}} \,. \tag{58}$$

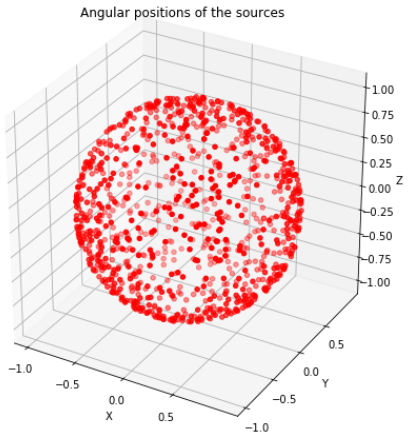

FIG. 4: Angular positions of the sources

Numerical simulations

In this section we test our method numerically, assuming there is no noise in the detectors. We choose $N = 1000$ sources randomly positioned in the sky (Fig. 4) with random amplitudes, phases and random frequencies normally distributed around a given mean value, see Fig. 5(b). The cross-correlator of two signals and the cross-spectrum are shown in Figs. 5(c)&5(d), respectively. The angular curves are obtained within the given frequency band and shown in Figs. 6(a)&6(b). The long-wavelength limit gives the identical result to the analytic formula Eq. (18), here $D_2 = 0.1\, D_1$ by choice. The short wavelength limit agrees with Eq. (18) within one standard deviation. It is interesting that Fig. 6(a) remains the same even for $N = 100$ sources.

TODO list:

- Add examples for Eq. (57), such as comparable (white?) noise for the clocks. Can take this integral at all? Aligned detectors? ACES?
- Can we replace T by ∞? What are the finite T errors? Read Hellings and Bertotti/Iess.
- Add references on Khoury and also on BEC DM with the possibility of very light fields. Perhaps, comment more on the gapless modes aka phonons and how this will change the derivation in the case of vector fields.
- Modify the theory part at the very beginning and merge it with the scalar case. Make sure it doesn't overlap with the previous paper.
- Emphasize the new points of the GW part
- Add description of the AI and cite 1707.04571
- Check the definition of the spectral power taking into account the number of polarizations
- Pulsar timing as a short-wavelength limit (recall the change in the rotation rate due to the change in the moment of inertia)

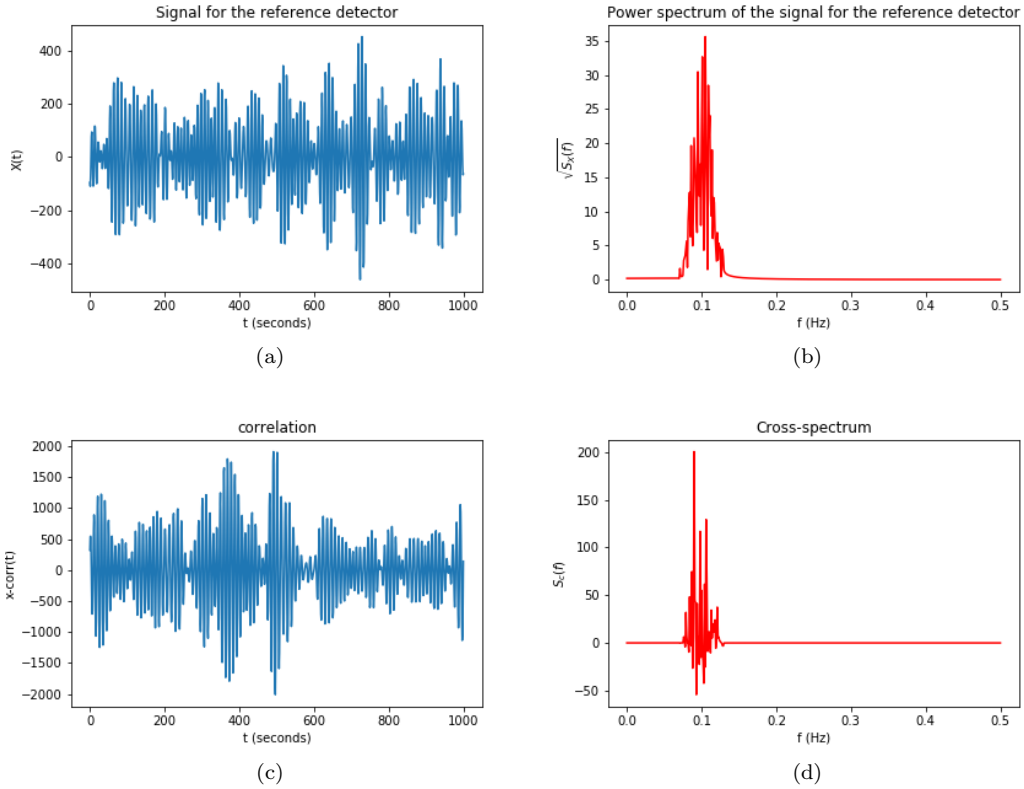

FIG. 5: (a) Signal at the reference detector (clock); (b) Its spectrum; (c) Correlator for two signals (two pairs of atomic clocks); (d) Cross-spectrum Fourier or from PYTHON sub-routine?.

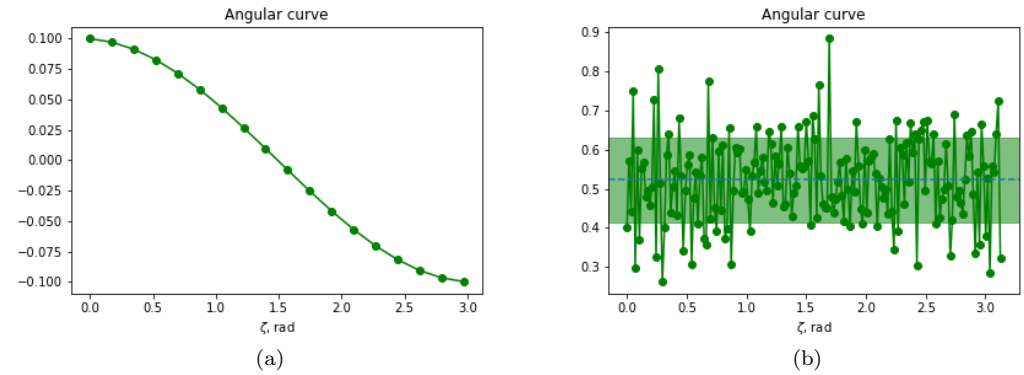

FIG. 6: Angular curves for the (a) long-wavelength background; (b) short-wavelength background. The band shows 1σ confidence interval for the constant value of $F(\zeta)$.

- Describe the measurement procedure in more detail. Justify some of the parameters through the simulation.
- Idea of the simulation: [A] there are 2 aligned detectors with high noise (1) Monochromatic wave (2) Stochastic background. Figure out the right sampling and duration of the experiment. [B] Reproduce the cross-correlation angular curve, similar to how it's done in Tempo2.

[1] T. Kalaydzhyan and N. Yu, arXiv:1705.05833 [hep-ph].
[2] T. Damour and J. F. Donoghue, Phys. Rev. D **82**, 084033 (2010)
[3] Y. V. Stadnik and V. V. Flambaum, Phys. Rev. Lett. **115**, no. 20, 201301 (2015)
[4] A. Derevianko, arXiv:1605.09717 [physics.atom-ph].
[5] A. Derevianko and M. Pospelov, Nature Phys. **10**, 933 (2014)
[6] A. Arvanitaki, J. Huang and K. Van Tilburg, Phys. Rev. D **91**, no. 1, 015015 (2015)
[7] A. Hees, J. Guna, M. Abgrall, S. Bize and P. Wolf, Phys. Rev. Lett. **117**, no. 6, 061301 (2016)
[8] V. V. Flambaum, D. B. Leinweber, A. W. Thomas and R. D. Young, Phys. Rev. D **69**, 115006 (2004)
[9] C. Patrignani *et al.* [Particle Data Group Collaboration], Chin. Phys. C **40**, no. 10, 100001 (2016).
[10] N. P. Pitjev and E. V. Pitjeva, Astron. Lett. **39**, 141 (2013) [Astron. Zh. **39**, 163 (2013)]
[11] P. W. Graham, D. E. Kaplan, J. Mardon, S. Rajendran and W. A. Terrano, Phys. Rev. D **93**, no. 7, 075029 (2016)
[12] P. Wcislo, P. Morzynski, M. Bober, A. Cygan, D. Lisak, R. Ciurylo and M. Zawada, Nature Astronomy **1**, 0009 (2016)
[13] A. Khmelnitsky and V. Rubakov, JCAP **1402**, 019 (2014)
[14] V. V. Flambaum and V. A. Dzuba, Can. J. Phys. **87**, 25 (2009)
[15] G. Prezeau, Astrophys. J. **814** (2015) no.2, 122
[16] R. w. Hellings and G. s. Downs, Astrophys. J. **265**, L39 (1983).
[17] F. A. Jenet and J. D. Romano, Am. J. Phys. **83**, 635 (2015)
[18] G. Gelmini and P. Gondolo, Phys. Rev. D **64**, 023504 (2001)
[19] W. J. Riley, "Handbook of Frequency Stability Analysis", National Institute of Standards and Technology (NIST), U.S. Department of Commerce, NIST Special Publication 1065, July 2008.
[20] B. Allen and J. D. Romano, Phys. Rev. D **59**, 102001 (1999)
[21] B. Allen, In "Les Houches 1995, Relativistic gravitation and gravitational radiation", 373-417 [gr-qc/9604033].
[22] J. D. Romano and N. J. Cornish, Living Rev. Rel. **20**, 2 (2017)
[23] L. A. Wainstein, V. D. Zubakov, "Extraction of signals from noise", Prentice Hall, Englewood Cliffs, NJ (1962).
[24] Hellings, Ronald W., Phys. Rev. D **23** 832 (1981)
[25] M. Anholm, S. Ballmer, J. D. E. Creighton, L. R. Price and X. Siemens, Phys. Rev. D **79**, 084030 (2009),
[26] Bertotti, B.; Iess, L., Gen. Rel. and Grav., vol. 17, Nov. 1985, p. 1043-1058.
[27] J. Gair, J. D. Romano, S. Taylor and C. M. F. Mingarelli, Phys. Rev. D **90** (2014) no.8, 082001 doi:10.1103/PhysRevD.90.082001 [arXiv:1406.4664 [gr-qc]].
[28] N. Yu and M. Tinto, Gen. Rel. Grav. **43**, 1943 (2011)
[29] S. Kolkowitz, I. Pikovski, N. Langellier, M. D. Lukin, R. L. Walsworth and J. Ye, Phys. Rev. D **94**, no. 12, 124043 (2016)
[30] P. Delva, C. Le Poncin-Lafitte, P. Laurent, F. Meynadier and P. Wolf, Highlights Astron. **16** (2015) 211 [arXiv:1206.6239 [physics.space-ph]].
[31] N. Leefer, A. Gerhardus, D. Budker, V. V. Flambaum and Y. V. Stadnik, Phys. Rev. Lett. **117**, no. 27, 271601 (2016)
[32] K. Van Tilburg, N. Leefer, L. Bougas and D. Budker, Phys. Rev. Lett. **115** (2015) no.1, 011802
[33] R. Tyumenev et al., New Journal of Physics, **18**, 113002 (2016)
[34] K. Yamanaka et al, Phys. Rev. Lett. **114** (2015), 230801
[35] T. Rosenband et al., Science **319** (2008), Issue 5871, pp. 1808-1812
[36] l. Galleani and P. Tavella, IEEE Trans. Ultrason. Ferroelectr. Freq. Control, vol. 56, no. 3, pp. 450 464, 2009.
[37] C. A. Greenhall, "Frequency stability review", Telecommunications and Data Acquisition Progress Report 42-88, Oct.-Dec. 1986, Jet Propulsion Laboratory.
[38] B. J. Bloom *et al.*, Nature **506**, 71 (2014)